

Supporting Information

Dual Enzyme-mimicking Carbon Dots for Enhanced Antibacterial Activity

Guiming Niu, Fucheng Gao, Can Li, Yandong Wang, Hui Li* and Yanyan Jiang*

Affiliations:

Key Laboratory for Liquid-Solid Structural Evolution and Processing of Materials, Ministry of Education, Shandong University, Jinan, 250061, China

Experimental Section

Material characterizations: The morphological information of Co-Lvx-CDs was obtained on the transmission electron microscope (TEM; HT-7700, HITACHI and FEI Titan3 Cubed 60-300). Fourier transform infrared spectrometer (Nicolet 6700, Thermo Scientific) was used to analyze the surface functional groups of the sample. X-ray photoelectron spectroscopy (ESCALAB 250Xi, Thermo Electron, USA) was used to confirm the chemical state of Co-Lvx-CDs. The pH meter used in the experiments is PHS-3C, from INESA Scientific Instrument Co., Ltd., China. The ultraviolet-visible spectrum was obtained from the UV-vis spectrophotometer (SPECORD 200 PLUS, Jena, Germany). The scanning confocal fluorescence imaging microscope (CLSM800, Carl Zeiss, Germany) was applied to observe the cell imaging. The morphology and surface microstructure of the products are examined using a scanning electron microscope (SEM) (TESCAN MIRA LMS, Czech Republic). Fluorescence images of bacterial uptake of Co-Lvx-CDs were taken by inverted fluorescence microscopy (IX73 Inverted fluorescence microscope, Olympus, China).

Supplementary Figures

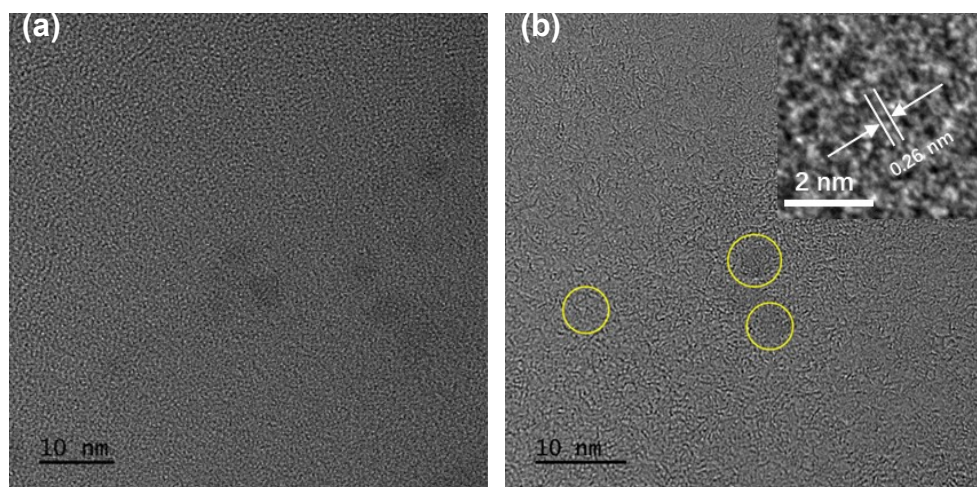


Fig. S1 TEM images of LvX-CDs.

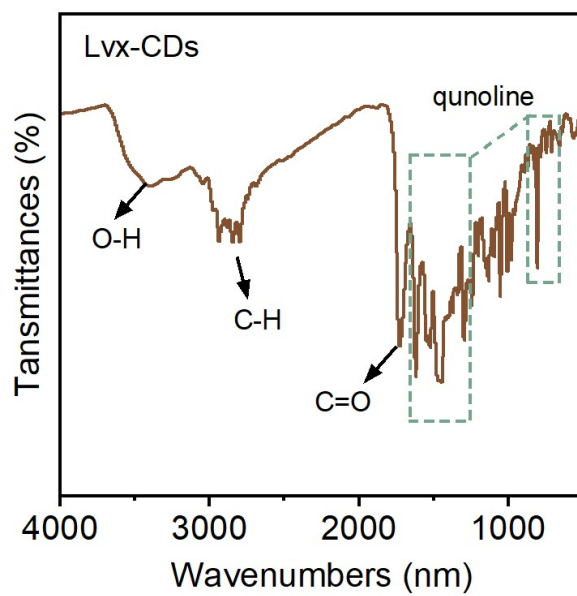


Fig. S2 FT-IR spectra of Lvx-CDs.

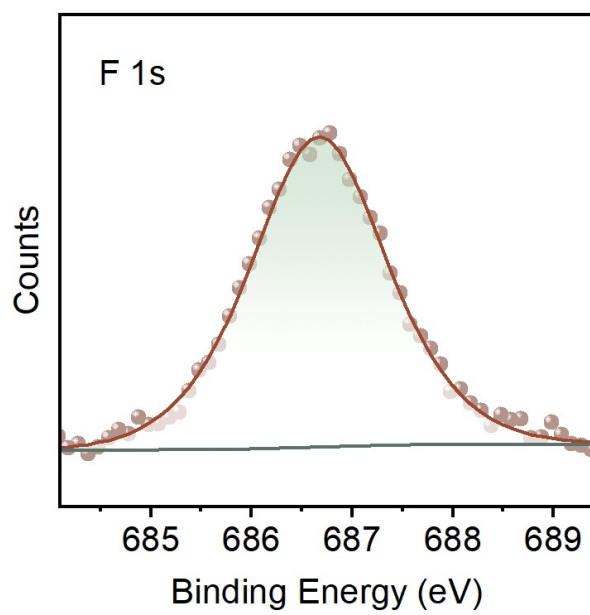


Fig. S3 XPS spectra of F 1s in Co-Lvx-CDs.

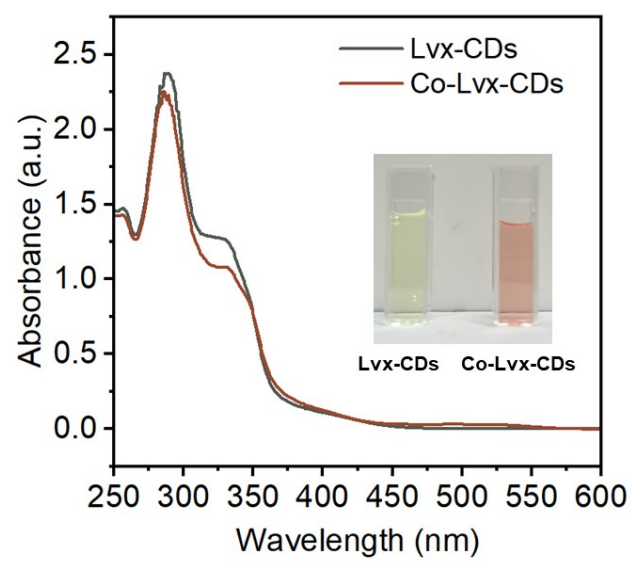


Fig. S4 The UV-Vis absorption spectrum of Co-Lvx-CDs and Lvx-CDs.

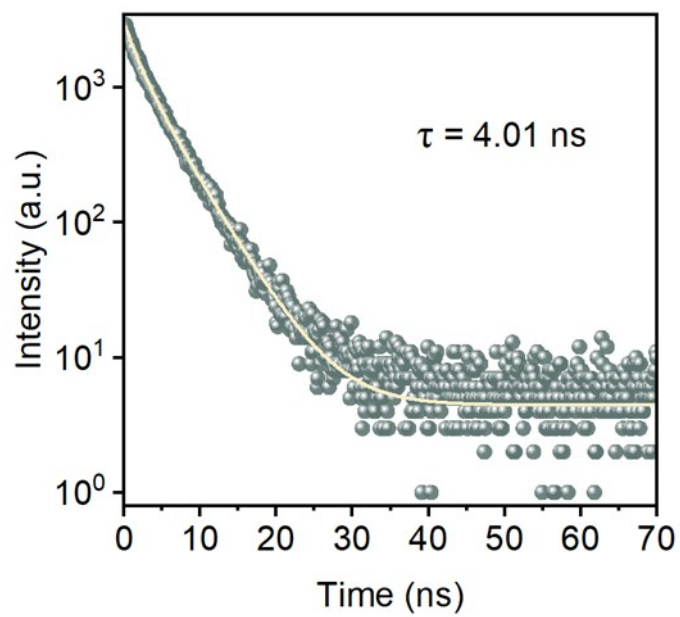


Fig. S5 The PL-decay curves of Lvx-CDs.

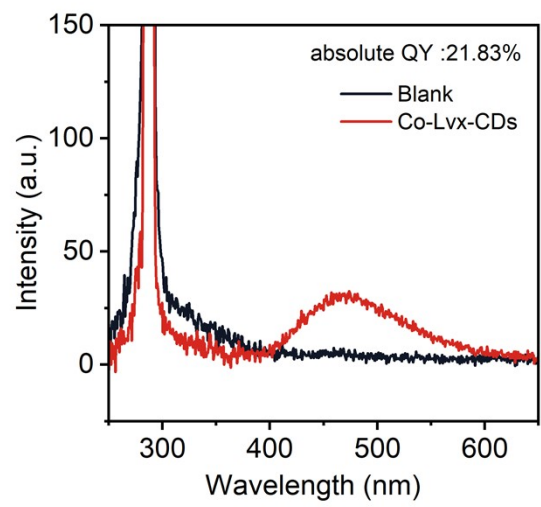


Fig. S6 Absolute fluorescence quantum yield map of Co-Lvx-CDs.

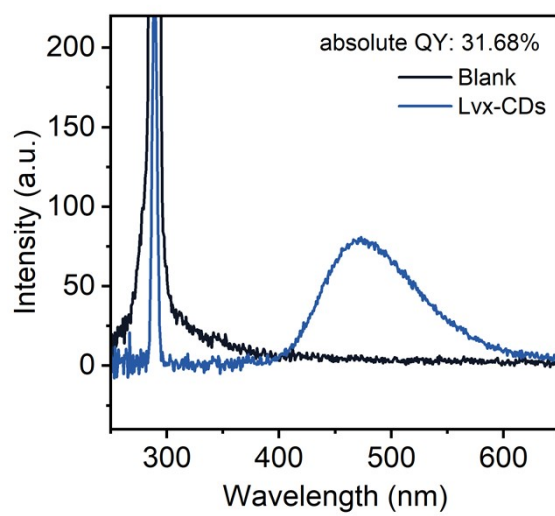


Fig. S7 Absolute fluorescence quantum yield map of LvX-CDs.

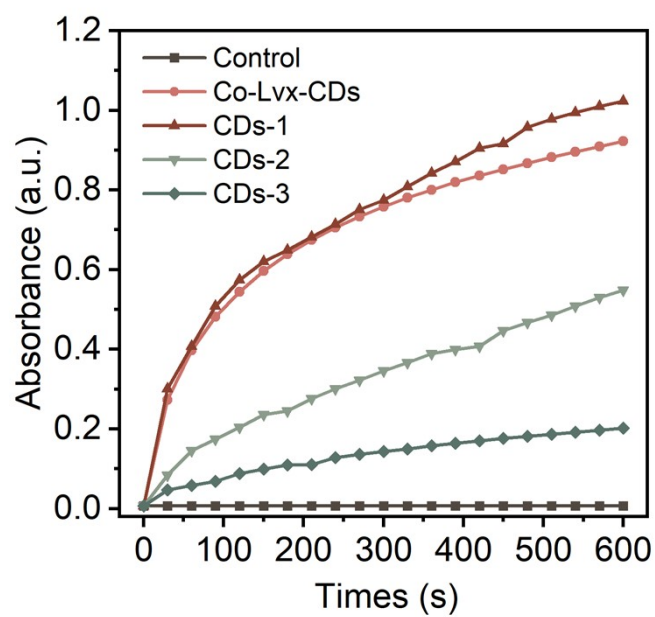


Fig. S8 “Absorbance-Time” curves of Co-doped CDs with different feed ratios as peroxidase. The concentration of CDs in the system were all 50 $\mu\text{g}/\text{mL}$ and the concentration of H_2O_2 was 500 μM . (CDs-1, Co-Lvx-CDs, CDs-2, and CDs-3 are corresponded to the ratio of levofloxacin to vitamin B12 is 3:1, 5:1, 7:1, and 9:1)

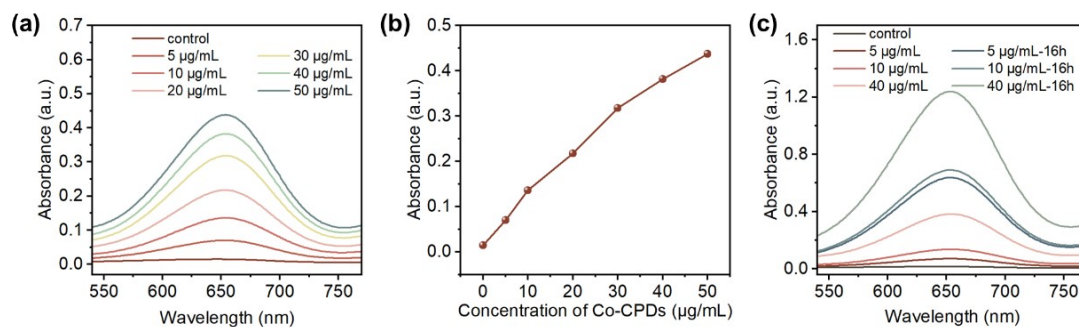


Fig. S9 The oxidase-like activity of Co-Lvx-CDs. (a) he absorption spectrums of TMB after 10 min reaction at different concentrations of Co-Lvx-CDs; (b) The Co-Lvx-CDs concentration-dependent ability of ROS production; (c) The absorbance of different concentrations of Co-Lvx-CDs continue to react for 16 hours compared with the 3 hours.

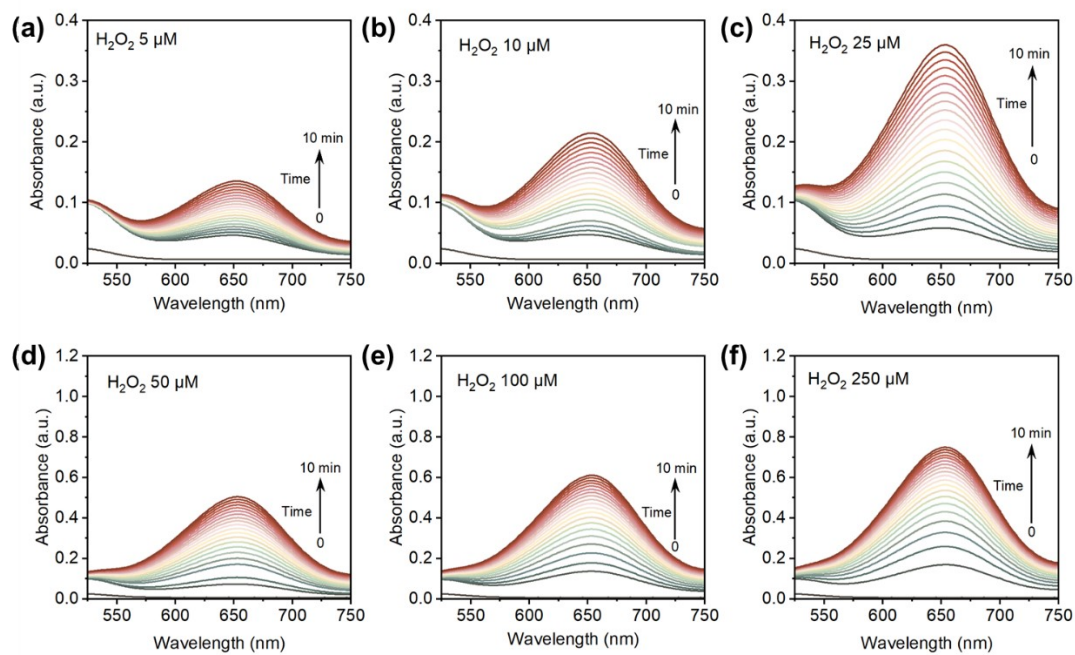


Fig. S10 The absorption spectra of TMB changes with time in 10 min under different concentrations of H_2O_2 .

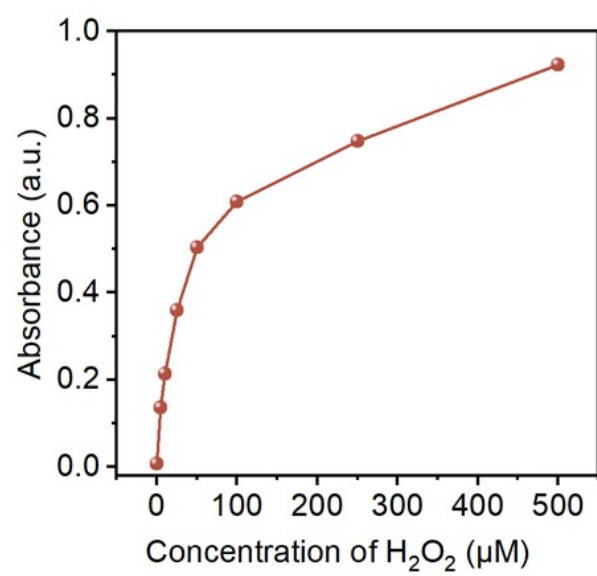


Fig. S11 The H₂O₂ concentration-dependent ability of ROS production.

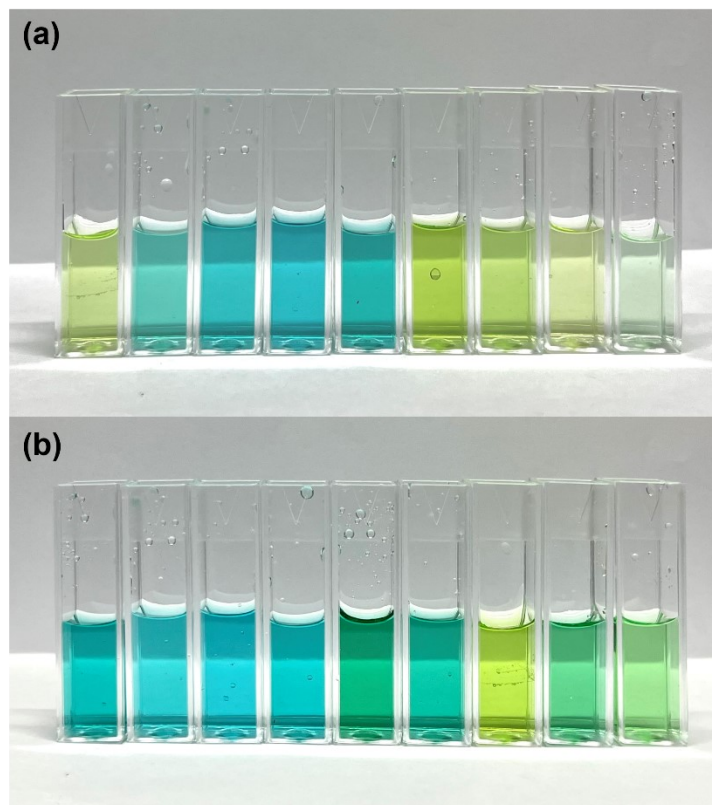


Fig. S12 Changes of TMB colour development at different temperatures. a Different color at 0, 10, 20, 30, 40, 50, 60, 70, 80 °C for 10 min; b Different color after 20 min of recovery to room temperature, respectively.

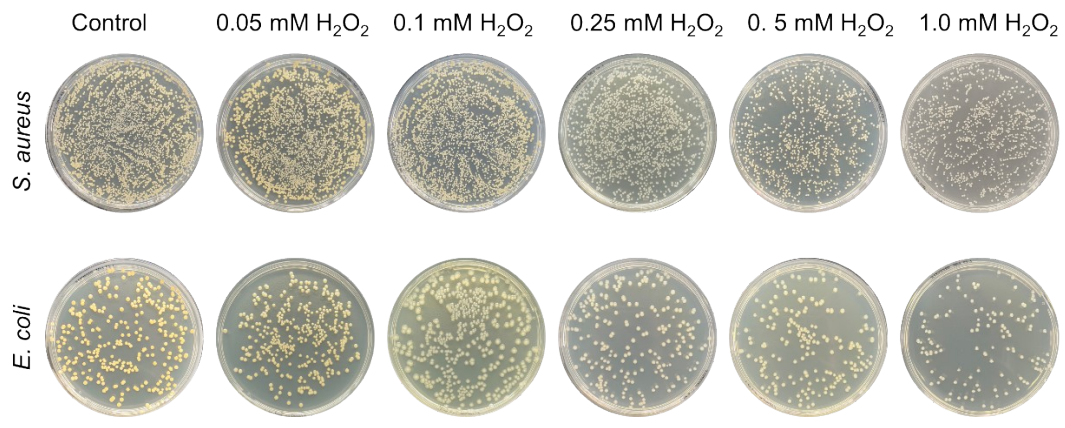


Fig. S13 Photographs of *S. aureus* and *E. coli* colonies treated with different concentrations of H₂O₂.

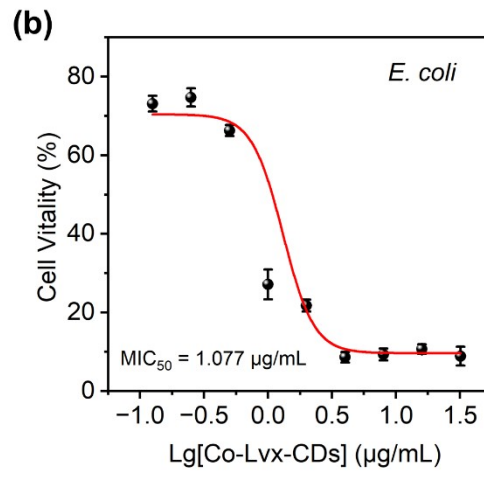
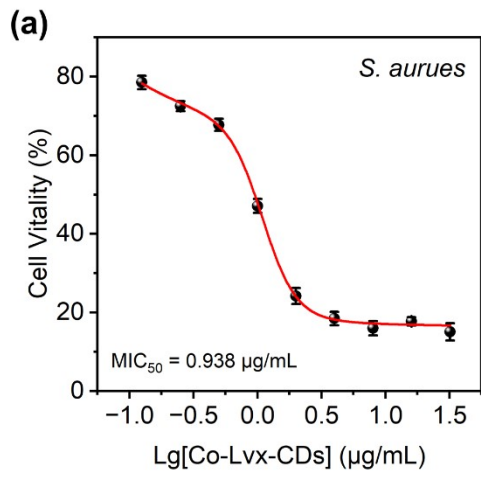


Fig. S14 The MIC_{50} of Co-Lvx-CDs. (a) The MIC_{50} curve for *S. aureus*. (b) The MIC_{50} curve for *E. coli*.

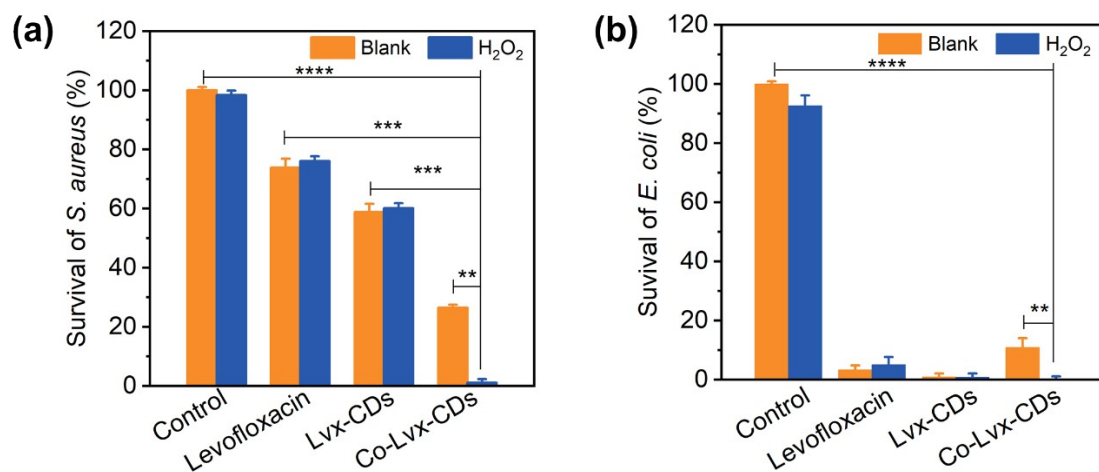


Fig. S15 Survival of (a) *S. aureus* and (b) *E. coli* treated with control, H₂O₂, levofloxacin, levofloxacin + H₂O₂, Lvx-CDS, Lvx-CDS + H₂O₂, Co-Lvx-CDS, and Co-Lvx-CDS+H₂O₂ (*p <0.05, **p <0.01, ***p <0.001, ****p <0.0001).

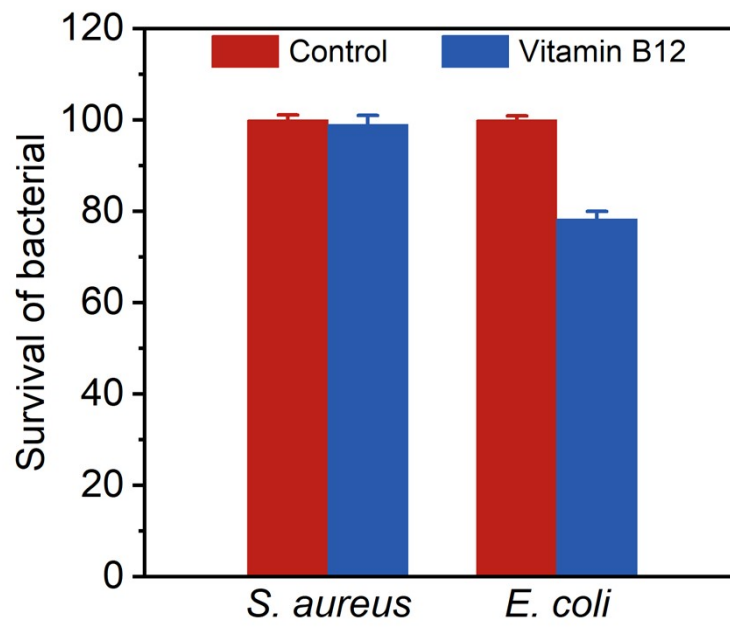


Fig. S16 Survival of *S. aureus* and *E. coli* treated with control and vitamin B12.

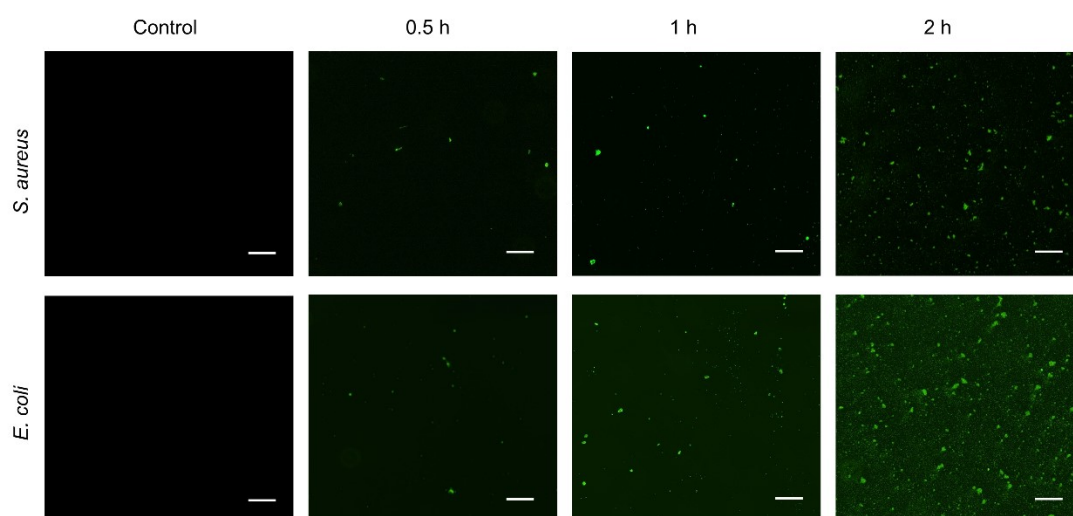


Fig. S17 Uptake of Co-Lvx-CDs by *S. aureus* and *E. coli* under fluorescence microscope (scale bar is 200 μm).

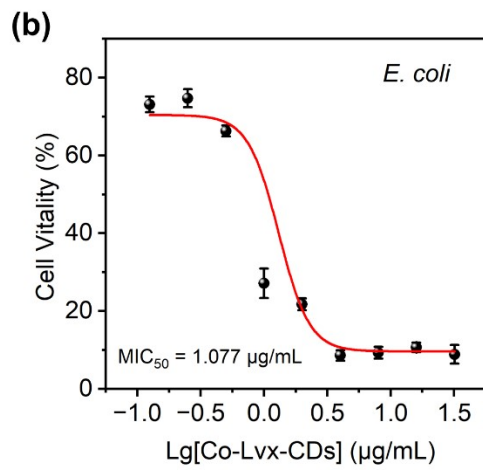
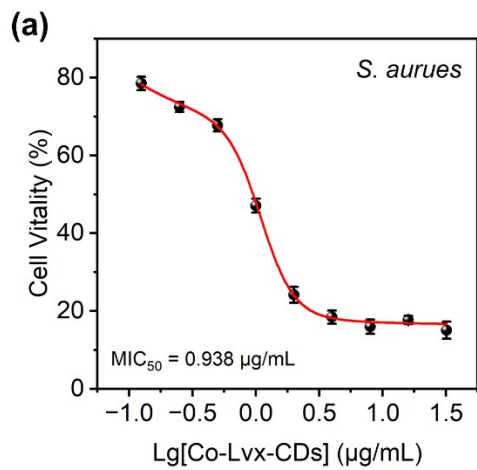


Fig. S18 The MIC_{50} Curve of Co-Lvx-CDs.

Supplementary Table

Table S1 The parameters about the steady-state kinetics of nanozymes.

Nanozyme	K_m (mM)	V_{max} (10^{-8} M/s)	References
Cu ₉ Bi ₁ aerogel	6.25	0.279	1
2D Cu-TCPP(Fe) MOFs	2.67	17.7	2
NTA@CS-CNS	378	0.01635	3
Cu, Cl-CDs	0.219	2.353	4
Fe-CDs	97.64	42.4	5
Co-Lvx-CDs	0.0728	6789.7	This work

Table S2 The minimum inhibitory concentration (MIC₅₀) of other nanomaterials.

Nanomaterials	MIC ₅₀ (µg/mL)		References
	<i>S. aureus</i>	<i>E. coli</i>	
CGNPs	1.6	1.39	6
BJ-AgNP	40	60	7
ZnO nanoparticle	45.6	312.5	8
HCu NPs	350	500	9
Co-Lvx-CDs	0.938	1.077	This work

References

- 1 T. Wang, J. Feng, H. Sun, Y. Liang, T. Du, J. Dan, J. Wang and W. Zhang, *Sensors and Actuators B: Chemical*, 2023, **379**, 133249.
- 2 Y. Zhou, B. Zheng, L. M. Lang, G. X. Liu and X. H. Xia, *Acs Applied Nano Materials*, 2022, **5**, 18761-18769.
- 3 A. K. Shukla, S. Randhawa, T. C. Saini and A. Acharya, *Int. J. Biol. Macromol.*, 2023, **233**, 123466.
- 4 N. Zhao, J. Song and L. Zhao, *Colloids and Surfaces a: Physicochemical and Engineering Aspects*, 2022, **648**, 129390.
- 5 Y. Liu, B. Xu, M. Lu, S. Li, J. Guo, F. Chen, X. Xiong, Z. Yin, H. Liu and D. Zhou, *Bioact. Mater.*, 2022, **12**, 246-256.
- 6 F. Alshammari, B. Alshammari, A. Moin, A. Alamri, T. Al Hagbani, A. Alobaida, A. Baker, S. Khan and S. Rizvi, *Pharmaceutics*, 2021, **13**, 1896.
- 7 A. Mondal, A. Mondal, K. Sen, P. Debnath and N. K. Mondal, *Environ. Sci. Pollut. Res.*, 2023, **30**, 16525-16538.
- 8 B. Lallo Da Silva, B. L. Caetano, B. G. Chiari-Andréo, R. C. L. R. Pietro and L. A. Chiavacci, *Colloids and Surfaces B: Biointerfaces*, 2019, **177**, 440-447.
- 9 T. Jayaramudu, K. Varaprasad, R. D. Pyarasani, K. K. Reddy, A. Akbari-Fakhrabadi, V. Carrasco-Sanchez and J. Amalraj, *Carbohydr. Polym.*, 2021, **254**, 117302.

